

See discussions, stats, and author profiles for this publication at: <https://www.researchgate.net/publication/221833631>

# Comparative DFT Study To Determine if $\alpha$ -Oxoaldehydes are Precursors for Pentosidine Formation

ARTICLE in THE JOURNAL OF PHYSICAL CHEMISTRY A · MARCH 2012

Impact Factor: 2.69 · DOI: 10.1021/jp2104165 · Source: PubMed

---

CITATIONS

5

READS

45

## 4 AUTHORS, INCLUDING:



Rasoul Nasiri

University of Brighton

23 PUBLICATIONS 89 CITATIONS

[SEE PROFILE](#)



Mansour Zahedi

Shahid Beheshti University

65 PUBLICATIONS 366 CITATIONS

[SEE PROFILE](#)



Ali A Moosavi-Movahedi

University of Tehran

521 PUBLICATIONS 5,475 CITATIONS

[SEE PROFILE](#)

# Comparative DFT Study To Determine if $\alpha$ -Oxoaldehydes are Precursors for Pentosidine Formation

Rasoul Nasiri,<sup>†</sup> Martin J. Field,<sup>‡</sup> Mansour Zahedi,<sup>\*,†</sup> and Ali Akbar Moosavi-Movahedi<sup>||</sup>

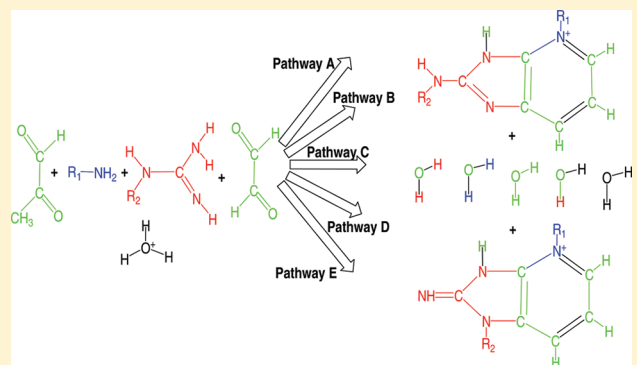
<sup>†</sup>Department of Chemistry, Faculty of Sciences, Shahid Beheshti University, Evin, 19839-63113, Tehran, Iran

<sup>‡</sup>DYNAMO Team, DYNAMOP Group, Institut de Biologie Structurale—Jean-Pierre Ebel, CNRS-CEA-UJF (UMRS075), Grenoble, France

<sup>||</sup>Institute of Biochemistry and Biophysics, University of Tehran, Tehran, Iran

## Supporting Information

**ABSTRACT:** We report a comprehensive density functional theory (DFT) study of the mechanism of pentosidine formation. This work is a continuation of our earlier studies in which we proposed pathways for formation of glucosepane (*J. Mol. Model.* **2011**, pp 1–15, DOI 10.1007/s00894-011-1161-x), GODIC (glyoxal-derived imidazolium cross-link), and MODIC (methyl glyoxal-derived imidazolium cross-link; *J. Phys. Chem.* **2011**, *115*, pp 13542–13555). Here we show that formation of pentosidine via reaction of  $\alpha$ -oxoaldehydes with lysine and arginine in aqueous solution is possible thermodynamically and kinetically, in good agreement with the available experimental evidence. Five pathways, A–E, were characterized, as in our previous GODIC and MODIC work. In pathways A and B, a Schiff base is first formed from lysine and methyl glyoxal (MGO), and this is followed by addition of arginine and glyoxal (GO). By contrast, in pathways C, D, and E, addition of arginine to MGO occurs first, resulting in the formation of imidazolone, which then reacts with lysine and GO to give pentosidine. Our calculations show that the reaction process is highly exergonic and that the three pathways A, C, and E are competitive. These results serve to underline the potentially important role that  $\alpha$ -oxoaldehydes play as precursors in pentosidine formation in the complex field of glycation.



## 1. INTRODUCTION

Experimental studies have shown that pentosidine is not only one of the major advanced glycation end-products (AGEs), but that it also serves as a useful biomarker for the study of glycoxidation processes *in vivo* and in food systems.<sup>1–9</sup> It is a fluorescent cross-link that is formed under oxidative conditions through reaction of lysine and arginine residues with hexoses, pentoses,<sup>10</sup> Amadori compounds,<sup>10a,c</sup> ascorbate,<sup>10a,c</sup> 3-deoxyglucosone (3-DG),<sup>10a</sup> and glyceraldehydes<sup>11</sup> and glycolaldehyde.<sup>12</sup> In addition, Litchfield et al. found that it can also be formed under nonoxidative conditions in their studies of pentose reactions.<sup>13</sup> Interestingly, in uremia (kidney or renal failure), the mechanism of pentosidine formation is related to two- and three-carbon carbohydrates and not to glucose, ribose, 3-DG, or ascorbic acid because pentosidine levels were the same between diabetic and nondiabetic hemodialysis subjects and the carbohydrate concentrations in uremic plasma were normal or low.<sup>3,13</sup> Moreover, aminoguanidine<sup>22</sup> and OPB-9195,<sup>23</sup> which are effective scavengers of  $\alpha,\beta$ -dicarbonyl compounds inhibited *in vitro* pentosidine formation in uremic plasma.<sup>3a</sup>

All these results, together with the availability and high reactivity of dicarbonyl compounds in human blood plasma,<sup>15,21</sup> imply a precursory role for  $\alpha$ -oxoaldehydes, such as glyoxal (GO) and methyl glyoxal (MGO), in uremic pentosidine

formation. Support for this came from Lapolla et al. who used GC-MS and LC techniques to investigate plasma and peritoneal dialysate in uremic patients and whose results indicated that GO and MGO were implicated in AGE formation.<sup>14</sup> By contrast, Biemel et al. ruled out involvement of two and three carbon products arising from ribose and glucose degradation in the formation of pentosidine in an *in vitro* model.<sup>20a</sup> However, the autodegradation of ribose and glucose to GO and MGO was shown to occur in buffered solution at 37 °C in another study,<sup>21</sup> and Miyata et al. found a precursory role for GO and MGO in pentosidine formation by using high-performance liquid chromatography and mass spectrometry techniques.<sup>3</sup> Interestingly, the latter results were obtained by incubating a fluid containing glucose (peritoneal dialysis (PD)) with bovine serum albumin (BSA).

These conflicting results led us to investigate possible mechanisms of formation of this important cross-link from  $\alpha$ -oxoaldehydes *in vivo* and in food systems. We performed density functional theory (DFT) calculations with the wB97XD functional to examine the pathways for pentosidine formation from GO, MGO, lysine, and arginine that are shown in

Received: October 30, 2011

Revised: February 1, 2012

Published: February 15, 2012

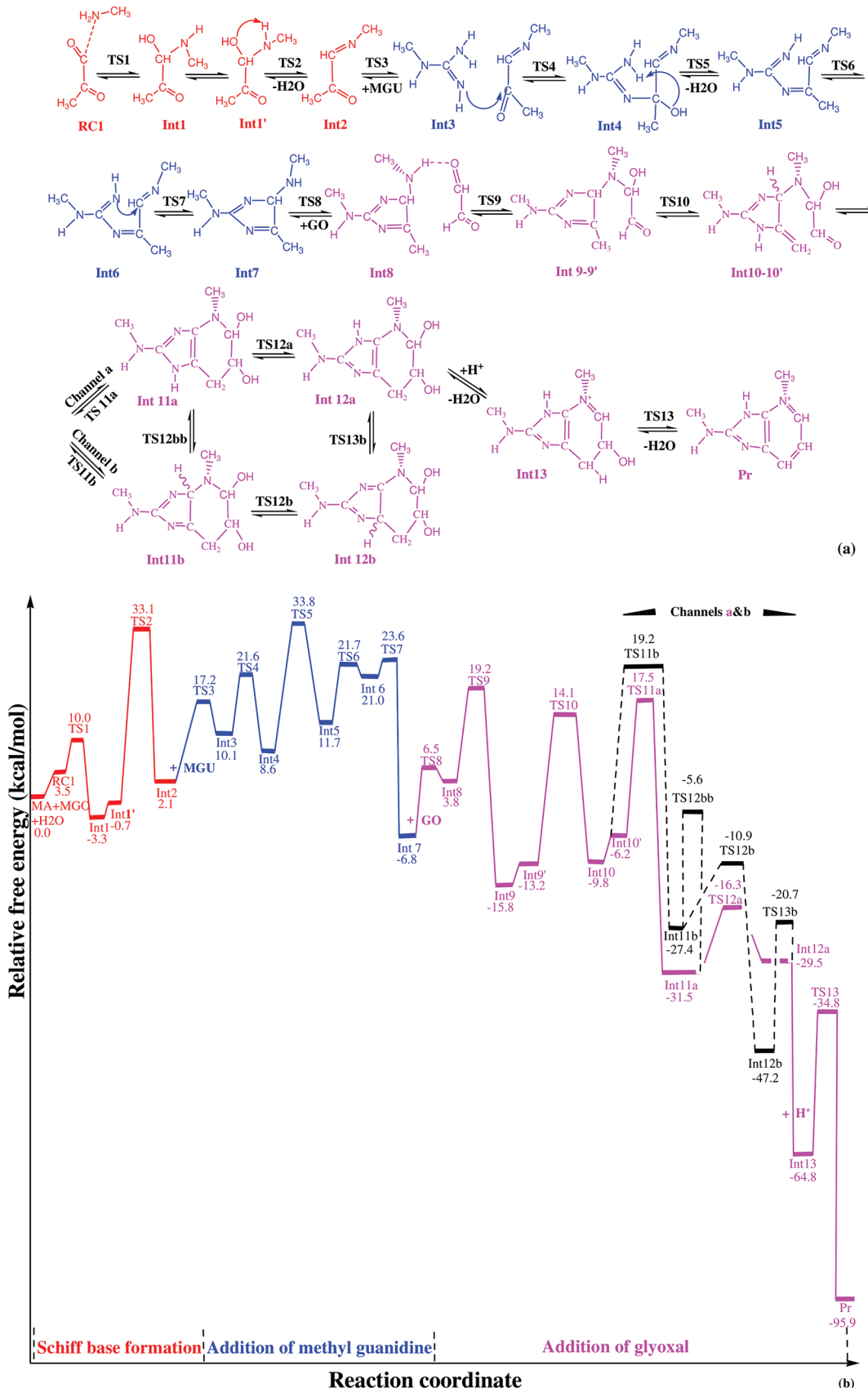


**Figure 1.** (a) Molecular steps of pentosidine formation in pathway A. (b) Free energy profile calculated at the CPCM/wB97XD/6-31+G\* level of theory in aqueous solution.

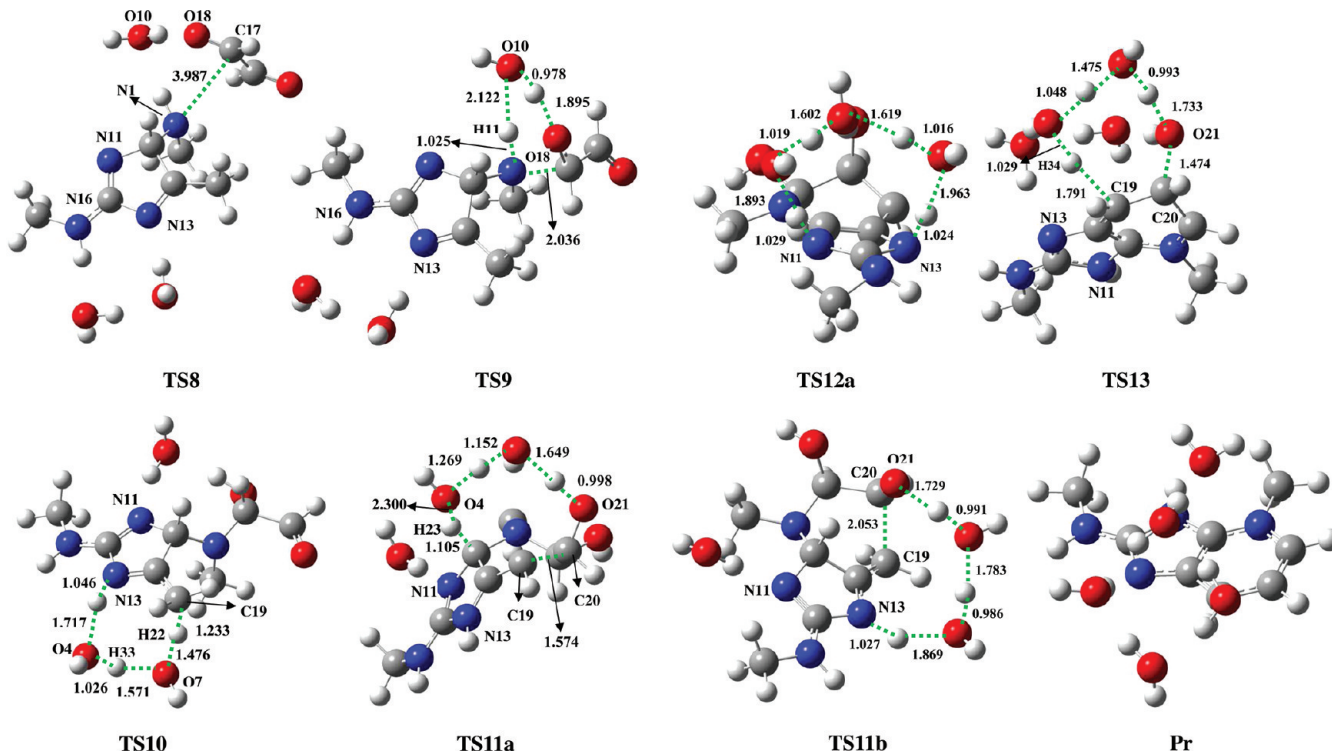


**Figure 2.** Structures of transition states and the final product from the third, addition of GO, stage of pathway A.

Figures 1a, 3a, 5a, 6a, and 8a. These pathways take advantage of the results of our previous work in which we studied GODIC (glyoxal-derived imidazolium cross-link) and MODIC(methyl glyoxal-derived imidazolium cross-link) formation.<sup>28</sup> Methyl amine (MA) and methyl guanidine (MGU) were selected as models of lysine and arginine residues to avoid complications due to conformational issues and to reduce computational expense. Solvent was represented both explicitly, by including up to five water molecules in the quantum chemical system, and implicitly using a solvent reaction field method.

Our calculations and the proposed mechanisms are in good agreement with the experimental findings of Litchfield et al.<sup>3</sup> and of Miyata et al.<sup>13</sup> and highlight the role of  $\alpha,\beta$ -dicarbonyl compounds in the formation of the pentosidine cross-link.

## 2. COMPUTATIONAL SCHEME

All calculations were done using the Gaussian 09 software<sup>16</sup> and the Gauss View program<sup>17</sup> for visualization. We employed a DFT method with the wB97XD functional<sup>18</sup> that includes empirical dispersion and is designed to provide an accurate treatment of nonbonded interactions and long-range correlation. The structures for all reactant complexes (RC), product complexes (Pr), intermediates (Int), and transition states (TS) were fully geometry optimized with the 6-31+G\* basis in the presence of water molecules. The structures and energies of selected structures along the pathways were then rerefined with a variable number of waters (1–5) and the larger 6-311++G\*\* basis. The latter is an effective choice that gives an accurate description of hydrogen transfer reactions and hydrogen-bonded species, especially when water molecules are involved in the cross-linking process.

Intrinsic reaction coordinate (IRC) calculations<sup>19a,b</sup> were employed to ensure the identity of the reactants and products corresponding to each TS structure. To evaluate the effects of water, we employed a cluster-continuum approach that made use of both a variable number of explicit water molecules and the implicit conductor-like polarized continuum model (CPCM).<sup>19c</sup> The latter is based on the solvent reaction field method (SCRF).<sup>19d</sup>

Vibrational analyses were performed on all optimized structures with the same functional and basis set as the corresponding geometry optimizations. All vibrational frequencies were left unscaled and used to obtain free energies at a temperature of 298 K. The free energy values for each step were computed using an ideal gas approximation with an effective, elevated pressure of 1354 atm. This value was derived from the experimental density of liquid water and is designed to reduce translation entropy, because translational motions are suppressed in solution.<sup>20</sup>

## 3. RESULTS AND DISCUSSION

We investigated five pathways, A–E, that we developed from equivalent pathways that we had elucidated in our previous work on GODIC and MODIC formation.<sup>28</sup> The relation between the previous pathways and the current ones are discussed in section 3.1, pathways A and B are discussed separately in sections 3.2 and 3.3, and pathways C, D, and E in section 3.4. All mechanisms are made up of three stages. In pathways A and B, the first two stages consist of formation of a Schiff base from lysine and MGO, followed by addition of arginine. In pathways C, D, and E, these stages are reversed so that addition of arginine to MGO occurs before lysine. The third stage in all of the mechanisms is the addition of GO to form pentosidine.

Schematics of the proposed mechanisms and energy diagrams are depicted for each pathway in Figures 1, 3, 5, 6,

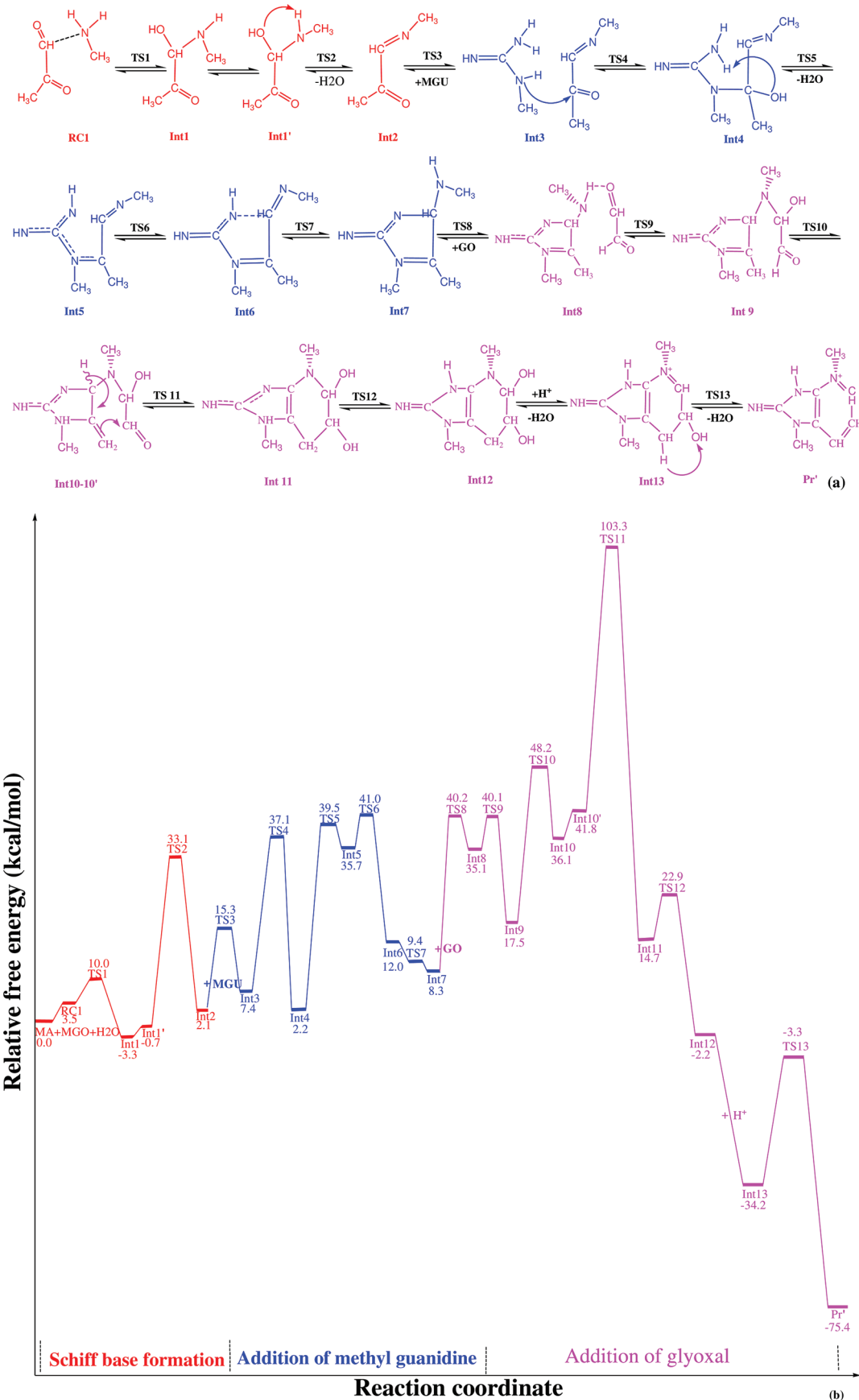


**Figure 3.** (a) Molecular steps of pentosidine formation in pathway B. (b) Free energy profile calculated at the CPCM/wB97XD/6-31+G\* level of theory in aqueous solution.

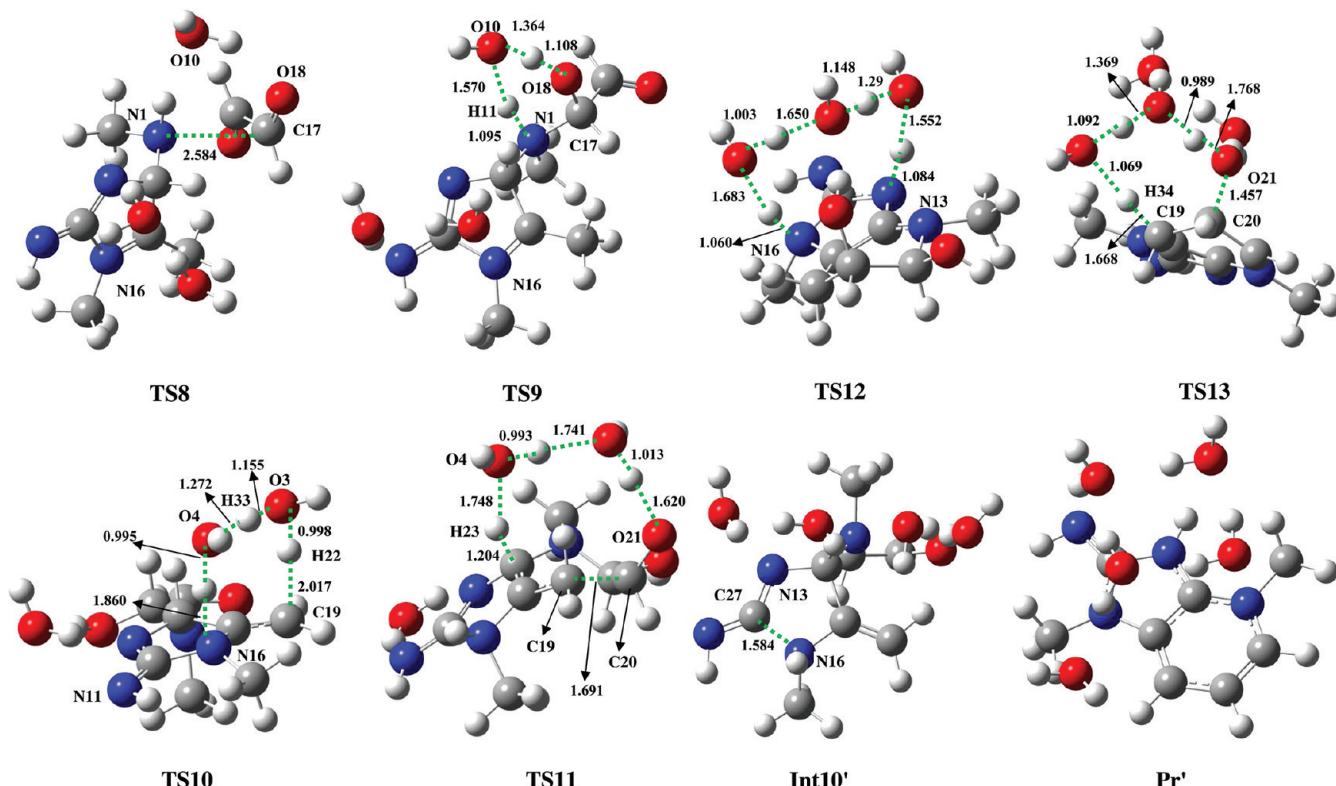


**Figure 4.** Structures of transition states, **Int10** and the final product from the third, addition of GO, stage of pathway B.

and 8, and some relevant structures are illustrated in Figures 2, 4, and 7. The free energy values for all stationary points in aqueous solution, calculated at the CPCM/wB97XD/6-31+G\* level of theory, are gathered in Table 1. In addition, certain critical, high-barrier steps along each pathway were recharacterized with the larger 6-311++G\*\* basis set and including a variable number of water molecules (1–5) near the reactive center. These refined values are presented in Table 2.

**3.1. Relation to Mechanisms of GODIC and MODIC.** In our earlier work on GODIC and MODIC formation,<sup>28</sup> we investigated five two-stage pathways, A–E, that we use as the basis for the pathways calculated here. This means that most of the structures for the first two stages of the new pathways correspond to those that we described previously and so we focus our discussion on the third stage mechanisms, namely, the addition of GO, in the following sections.

In our GODIC and MODIC studies, we found that pathways A, C, and E were the preferred pathways, as they were thermodynamically and kinetically the most feasible.<sup>28</sup> We did this by performing initial scans of the mechanisms using the 6-31+G\* basis set without explicit water molecules, except those that were directly implicated in the reaction process. Subsequently, we selected a crucial high energy intermediate and TS structures along each of the pathways and carried out calculations with the larger 6-311++G\*\* basis and incorporated up to five explicit water molecules, as well as implicit solvent, into the structural optimizations. In pathways A, C, and E, these calculations resulted in significant reductions in the reaction barriers, whereas in pathways B and D there was little effect (see Table 2 of ref 28). We followed the same basic strategy as this for the addition of

GO in this work, with the energies that resulted for the smaller and larger basis set calculations being given in Tables 1 and 2, respectively.

**3.2. Pathway A: Schiff Base Formation and Exocyclic Addition of Methyl Guanidine and Glyoxal.** The novel, addition of GO, portion of this pathway starts at **Int7**, which is a five-membered heterocycle. The first reaction involves the correct positioning of GO with respect to **Int7** to form a complex **Int8**. Overall, the process is endergonic and occurs via **TS8**, with an activation free energy of 13.3 kcal/mol (Figure 1). The distance between the N1 and C17 atoms in the TS structure is 3.98 Å (Figure 2).

N1 in **Int8** must be deprotonated before it can attack the carbonyl group of GO. This is done with the help of the water molecule, which, thanks to hydrogen bonds with O18 and H11, acts as a bridge to facilitate the proton transfer via the concerted TS, **TS9**, with a free energy barrier of 15.4 kcal/mol. The first carbinolamine product of this transfer, **Int9**, undergoes a small conformational rearrangement to give **Int9'** and then forms an enamine, **Int10**, by transfer of the acidic proton, H22, to N13. The activation barrier for this step is 29.9 kcal/mol via **TS10**. However, this barrier decreased by, on average, 11 kcal/mol when its structure was refined with extra water molecules (see Table 2).

Once the enamine is formed, cyclization can occur. This may occur via two channels that we denote as channels a and b (see Figures 1a,b). This is a complicated step involving carbon–carbon bond formation and a concerted proton transfer. In channel a, the latter results in H23 being shuttled to O21 (see **TS11a** in Figure 2) around an unstrained 10-membered ring, formed in part by two water molecules that assist the proton transfer. The ring-closing distance between C19 and C20 in the

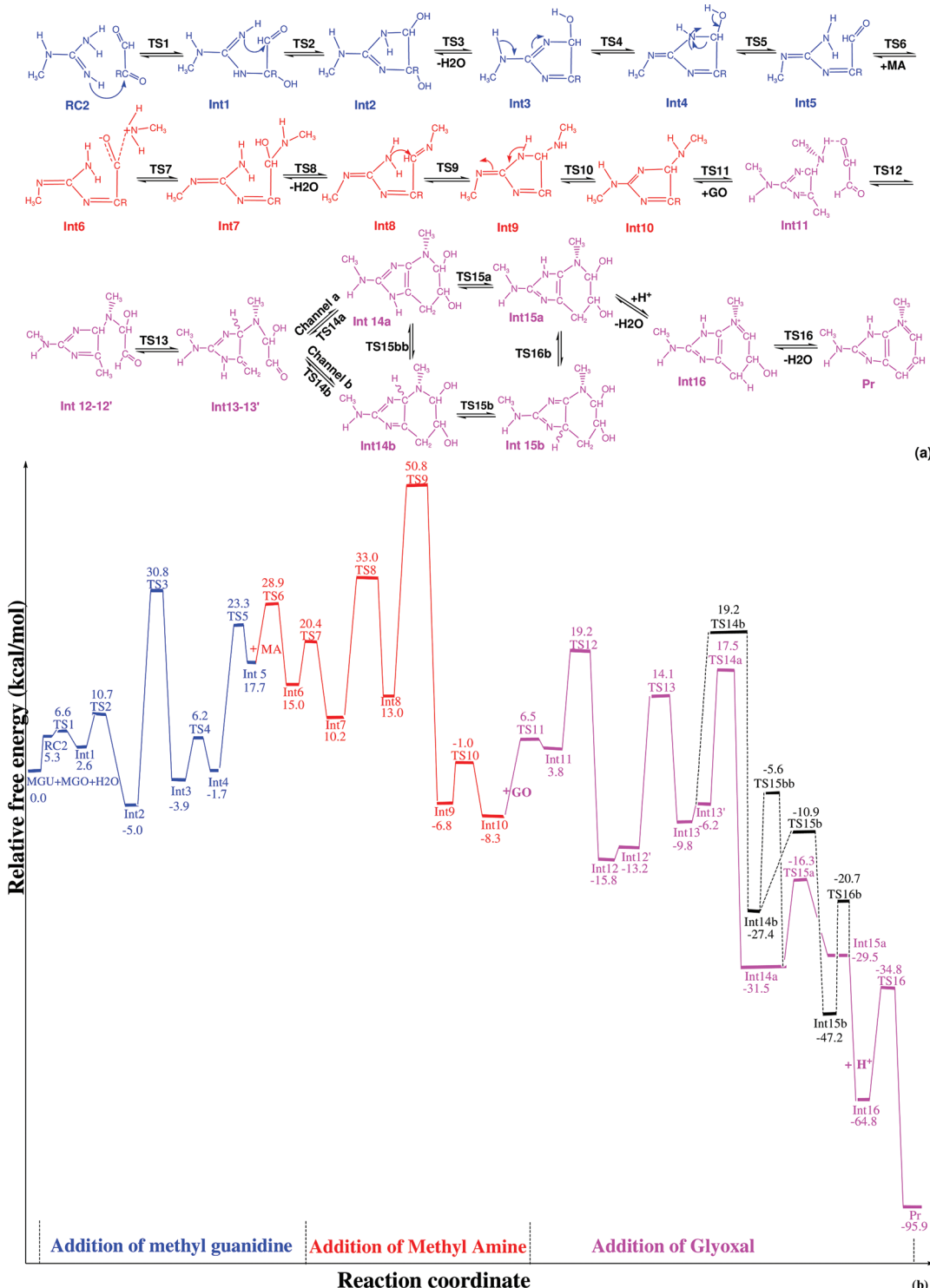


**Figure 5.** (a) Molecular steps of pentosidine formation in pathway C. (b) Free energy profile calculated at the CPCM/wB97XD/6-31+G\* level of theory in aqueous solution.

TS is 1.57 Å, and the activation barrier is 23.7 kcal/mol with respect to **Int10'**. After **TS11a**, the reaction proceeds downhill to **Int11a**, which is a six-membered heterocyclic ring attached to a five-membered one and which is 25.3 kcal/mol more stable than **Int10'**. The type of addition reaction involving enamines seen here has been observed in previous studies, notably in the Morita–Baylis–Hillman reaction and in the mechanism of direct aldol reactions catalyzed by amino amide derivatives.<sup>24,25</sup>

As reported in the literature,<sup>11,26a</sup> cyclization is followed by a proton transfer between the two exocyclic nitrogen atoms in the guanidine group from N13 to N11. This reaction occurs via **TS12a**, with an activation free energy of about 15 kcal/mol.

There is an alternative channel to the previous one, channel **b**, that starts from **Int10'** but which involves the transfer of the hydrogen from N13 to O21 instead of H23, again via two water

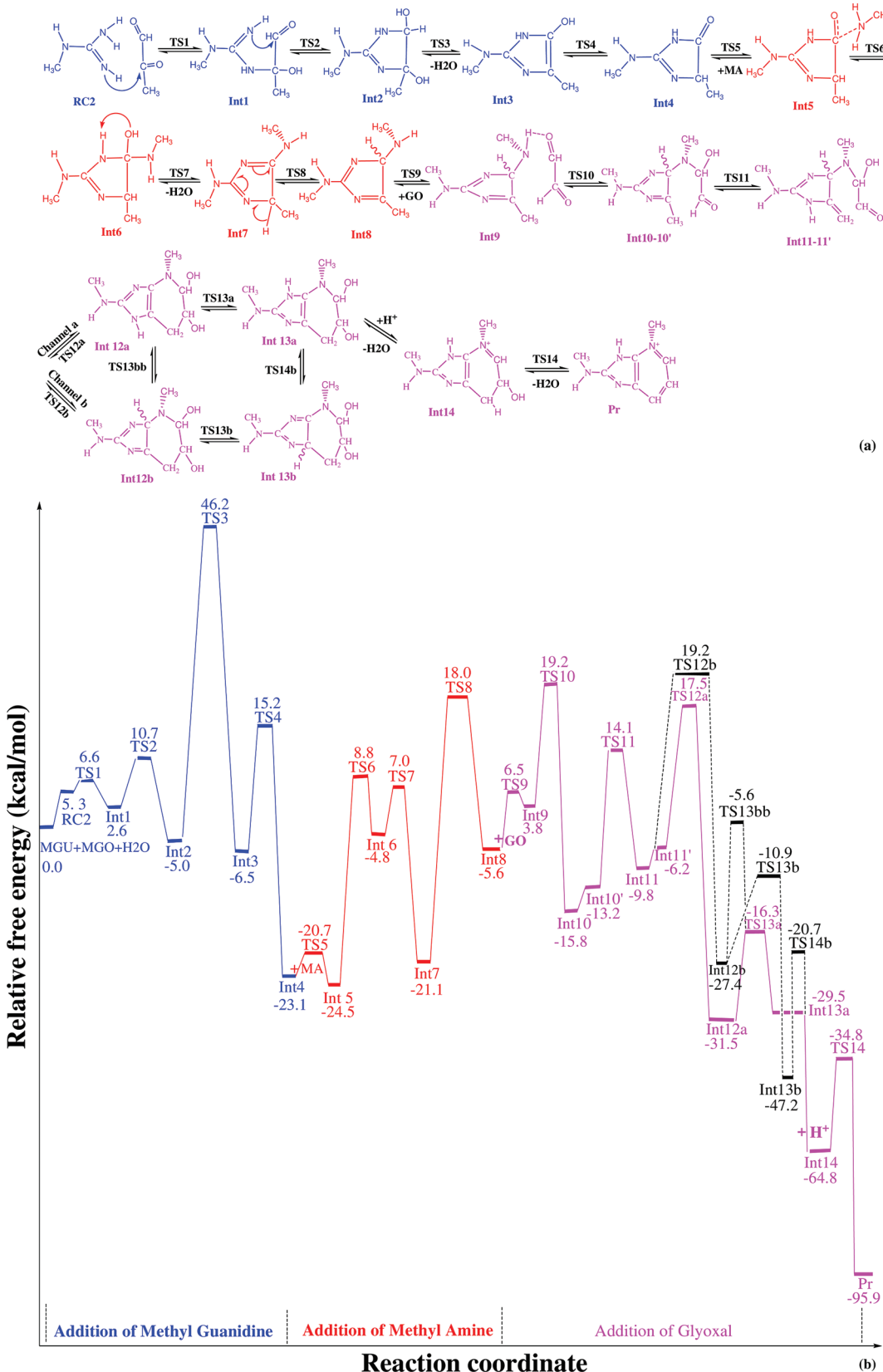


**Figure 6.** (a) Molecular steps of pentosidine formation in pathway D. (b) Free energy profile calculated at the CPCM/wB97XD/6-31+G\* level of theory in aqueous solution.

molecules (see TS11b in Figure 2). The barrier for this cyclization step is slightly higher than in channel a by 1.7 kcal/mol and the product, Int11b, is less stable than Int11a by 4.1 kcal/mol. Once Int11b is formed, there are two pathways for

its transformation into Int12a, both of which consist of two consecutive intramolecular proton transfers. The barriers for these steps are comparable, although overall larger, to that leading to Int12a from Int11a in channel a.

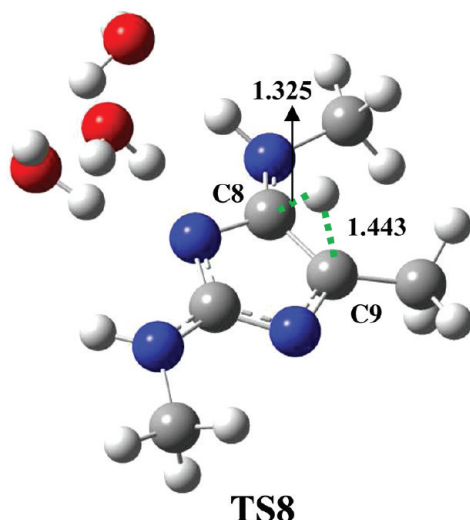


**Figure 7.** Structure of the last transition state from the second stage of pathway D.

Once **Int12a** is formed via either channels a or b, the next step involves addition of acid, as experiments have shown that pentosidine is stable against conventional acidic hydrolysis of proteins (6 M HCl, 110 °C, 24 h), whereas other cross-links (GODIC, MODIC, and glucosepane) are labile under these conditions.<sup>26</sup> Addition of acid to **Int12a** leads to the stable intermediate, **Int13**, which is 35.3 kcal/mol lower in energy than **Int12a**. The pathway terminates with a last dehydration, from **Int13** to the final product, Pr. The barrier is quite substantial, 30.0 kcal/mol, but the reaction is overall very exergonic.

As can be seen from Figure 1b, the highest activation barriers for the addition of GO are roughly equivalent to those from the other steps in the mechanism. Taking into account the barriers calculated with the higher level of theory and variable numbers of water molecules from Table 2 and their equivalents from ref 28, it appears that the dehydration reaction in GO addition (TS13) is rate-limiting. The overall process is very exergonic ( $\Delta G^\ddagger = -95.9$  kcal/mol), much more so than the equivalent values that we found earlier for glucosepane formation and for GODIC and MODIC (24.8, 25.0, and 15.6 kcal/mol, respectively). This is due in part to the  $\pi$ -electron resonance in the two connected rings, which lead pentosidine to have a high stability.

**3.3. Pathway B: Endocyclic Addition of Methyl Guanidine in Formation of Another Homologue of Pentosidine.** In our studies of MODIC formation, we derived pathway B to see if endocyclic, as opposed to exocyclic, addition of MGU to the Schiff base derived from MGO and lysine was possible. We found the pathway to be energetically unfavorable, in agreement with the experimental observation that endocyclic addition does not occur.

Nevertheless, we wanted to test whether addition of GO could occur to the relevant five-membered heterocycle intermediate, **Int7**, along pathway B and which is equivalent to the similar **Int7** from pathway A. It is to be noted that it is in principle possible to transform the two intermediates into each other via a methyl shift. However, the barrier for this process is very high, being 82.9 and 67.2 kcal/mol for the endomethyl shift (pathway A to B) and exomethyl shift (pathway B to A), respectively.

The broad outlines of the addition of GO are similar to those of pathway A. Thus, a reactive complex between GO and **Int7** must form first. This is more difficult than the equivalent steps of pathway A as the process is endergonic (26.8 kcal/mol) with a significant free energy barrier (31.9 kcal/mol). In the TS for the process, **TS8**, the N1 and C17 distance is 3.52 Å (Figure 4). The next step involves proton transfer and carbon–nitrogen bond formation and occurs, via **TS9**, with a barrier of 5.0 kcal/mol. Overall, the reaction is exergonic, and **Int9** is 17.6 kcal/mol more stable than **Int8**. However, the stability of **Int9** in pathway A is 33.3 kcal/mol more than the one in pathway B. After this, there is tautomerization of an amine to an enamine produced by transfer of the proton H22 from C19 to N16. The step is endergonic with a free energy barrier of 30.7 kcal, which is about 4 kcal/mol higher than the equivalent step in pathway A. The resulting enamine, **Int10**, is unstable as its five-membered cycle contains a C27–N16 bond with a distance of 1.60 Å (in contrast to the 1.38 Å found in pathway A; see Figure 4).

The second cyclization along the pathway involves shuttling of H23 to O21 via two water molecules, in addition to carbon–carbon bond formation. The barrier for this process is extremely high ( $\Delta G^\ddagger = 61.5$  relative to **Int10'**), to be compared with the much lower value obtained for pathway A ( $\Delta G^\ddagger = 23.7$  relative to **Int10'**). Adding more water molecules does not lower the barrier significantly (see Table 2), which indicates that water itself cannot facilitate this reaction. After **Int11**, there is transfer of a proton from N16 to N13 via **TS12**, which occurs with a low barrier of 8.2 kcal/mol, because population analysis shows that N16 has a large positive charge (0.6). The two last steps, which terminate the reaction, are broadly similar to those in pathway A, although the product is slightly different.

Comparison of the free energy profiles of pathways A and B shows that the latter is very unfavorable. This is due, in part, to the charge distribution in the five-membered ring of pathway B, because the positive charge on N16 found in the intermediates from **Int5** to **Int10** leads to destabilization of the ring. In pathway A, the values are always negative. In addition, **Int8** in pathway A is much more stable than that in pathway B because the two water molecules can hydrogen bond with the hydrogen from N16 and the nitrogen of N13 in imidazole ring, whereas in pathway B this is not possible due to the presence of the methyl group on N16 in MGU.

**3.4. Pathways C, D, and E.** Pathway C involves ring-opening of dihydroxyimidazolidine and addition of MA and GO, and pathway E involves successive dehydration reactions of dihydroxyl-imidazolidine (DHIm). The initial parts of both of these pathways are identical to those of pathways C and E for MODIC formation from our earlier study. After this, addition of GO occurs in an identical manner to that described for pathway A. This takes place from **Int10** in pathway C and from **Int8** in pathway E. As we saw for pathway A, this stage of the reaction is highly exergonic and has energy barriers that are less than or at most comparable to those of the preceding steps. Thus, addition of GO does not affect the feasibility of these mechanistic routes.

Pathway D corresponds to dehydration of dihydroxyimidazolidine obtained from MGU and MGO. Like the previous pathways, the first steps, up to **Int7**, are equivalent to those found in our previous study.<sup>28</sup> Equally, the addition of GO occurs in the same way to that of pathway A. However, to join the two, it is necessary to insert an additional step that

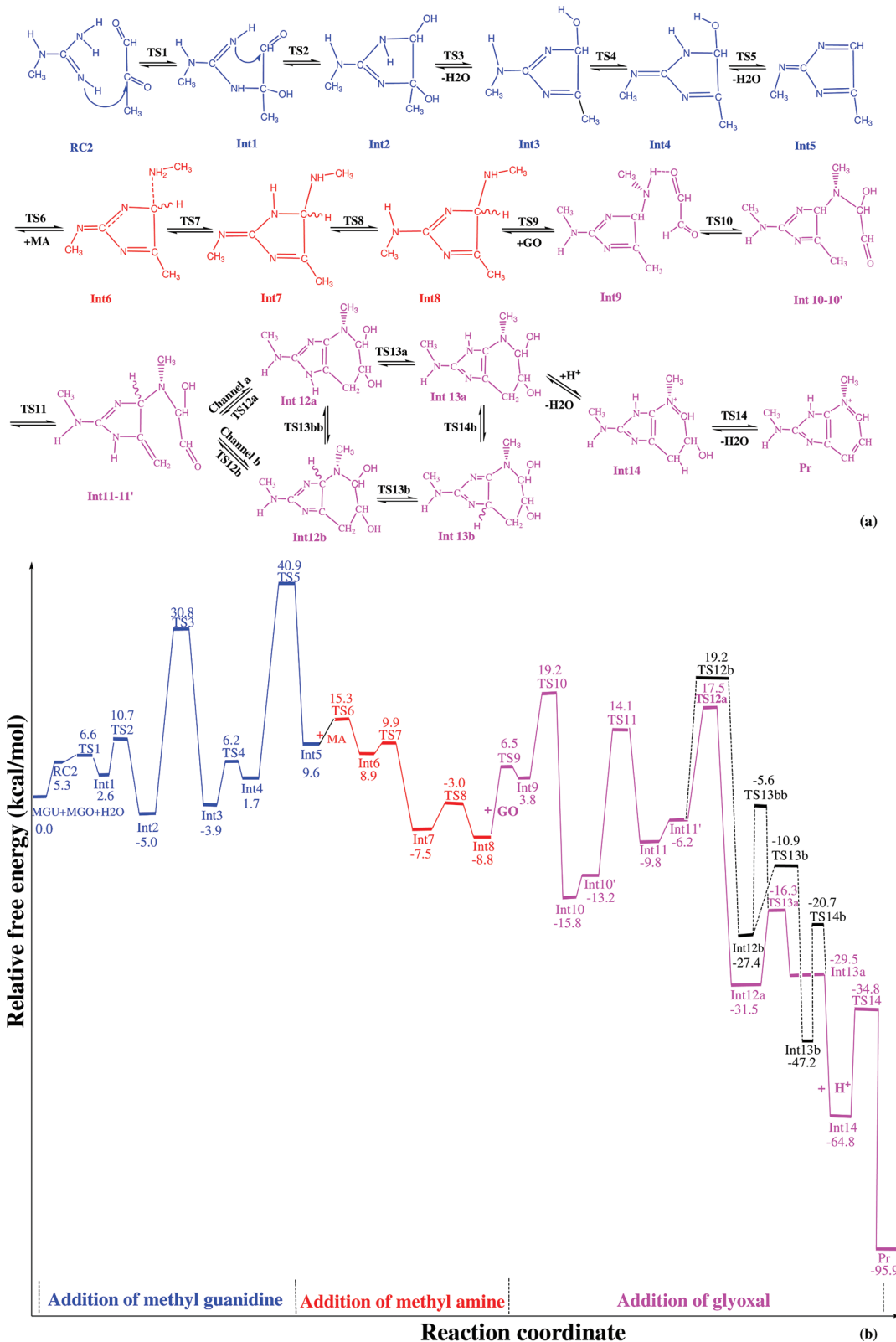


Figure 8. (a) Molecular steps of pentosidine formation in pathway E. (b) Free energy profile calculated at the CPCM/wB97XD/6-31+G\* level of theory in aqueous solution.

creates the correct five-membered heterocycle intermediate, **Int8**. This is done via an internal proton transfer from C9 to C8 (see **TS8** in Figure 7), which has a very high energy barrier of 39.1 kcal/mol (Figure 6). We sought, but were

unable to find, TS structures involving extra waters that greatly reduced this barrier, implying that water cannot facilitate this step and confirming that this mechanism is unlikely to be preferred.

**Table 1.** Relative Free Energies (in kcal/mol)<sup>a</sup> for Stationary Points Involved in the Cross-Linking Reaction of Pentosidine in Solution<sup>b</sup>

	pentosidine				
	path A	path B	path C	path D	path E
MGO + MA + MGU + GO	0.0	0.0	0.0	0.0	0.0
RC	3.5	3.5	5.3	5.3	5.3
TS1	10.0	10.0	6.6	6.6	6.6
Int1	-3.3	-3.3	2.6	2.6	2.6
Int1'	-0.7	-0.7			
TS2	33.1	33.1	10.7	10.7	10.7
Int2	2.1	2.1	-5.0	-5.0	-5.0
TS3	17.2	15.3	30.8	46.2	30.8
Int3	10.1	7.4	-3.9	-6.5	-3.9
TS4	21.6	37.1	6.2	15.2	6.2
Int4	8.6	2.2	-1.7	-23.1	1.7
TS5	33.8	39.5	23.3	-20.7	40.9
Int5	11.7	35.7	17.7	-24.5	9.6
TS6	21.7	41.0	28.9	8.8	15.3
Int6	21.0	12.0	15.0	-4.8	8.9
TS7	23.6	9.4	20.4	7.0	9.9
Int7	-6.8	8.3	10.2	-21.1	-7.5
TS8	6.5	40.2	33.0	18.0	-3.0
Int8	3.8	35.1	13.0	-5.6	-8.8
TS9	19.2	40.1	50.8	6.5	6.5
Int9	-15.8	17.5	-6.8	3.8	3.8
Int9'	-13.2				
TS10	14.1	48.2	-1.0	19.2	19.2
Int10	-9.8	36.1	-8.3	-15.8	-15.8
Int10'	-6.2	41.8		-13.2	-13.2
TS11	17.5 (19.2) <sup>c</sup>	103.3	6.5	14.1	14.1
Int11	-31.5 (-27.4)	14.7	3.8	-9.8	-9.8
Int11'				-6.2	-6.2
TS12	-16.3 (-10.9)	22.9	19.2	17.5 (19.2)	17.5 (19.2)
Int12	-29.5 (-47.2)	-2.2	-15.8	-31.5 (-27.4)	-31.5 (-27.4)
Int12'			-13.2		
TS13	-34.8 (-20.7)	-3.3	14.1	-16.3 (-10.9)	-16.3 (-10.9)
Int13	-64.8	-34.2	-9.8	-29.5 (-47.2)	-29.5 (-47.2)
Int13'			-6.2		
TS14			17.5 (19.2)	-34.8 (-20.7)	-34.8 (-20.7)
Int14			-31.5 (-27.4)	-64.8	-64.8
TS15			-16.3 (-10.9)		
Int15			-29.5 (-47.2)		
TS16			-34.8 (-20.7)		
Int16			-64.8		
Pr	-95.9	-75.4	-95.9	-95.9	-95.9

<sup>a</sup>Calculations were done at the CPCM/wB97XD/6-31+G\* level of theory. <sup>b</sup>Water has been used as the solvent. <sup>c</sup>The values in parentheses are for channel b in the third stage of the reaction.

#### 4. CONCLUSIONS

Pentosidine is an important biomarker and cross-link in vivo and in food systems. In this study, we investigated the mechanism of its formation from  $\alpha$ -oxoaldehydes and lysine and arginine using DFT calculations at the CPCM/wB97XD/6-31+G\* level of theory. We evaluated five pathways, A–E, the initial parts of which are identical to those that we elucidated in our earlier work on GODIC and MODIC formation.<sup>28</sup> As in our previous study, pathways A, C, and E were found to be energetically preferred. By contrast, pentosidine formation is much more exergonic than the other cross-links that we have investigated, whether

GODIC, MODIC, or glucosepane,<sup>27,28</sup> and the rate-limiting step in the pathway corresponds to the final dehydration step of GO addition. The other pathways, B and D, are kinetically disfavored due to the very high energy barriers that occur in both the initial stages of the reaction and in the addition of GO.

In summary, we have elucidated reaction pathways that suggest that formation of pentosidine from  $\alpha$ -oxoaldehydes, lysine, and arginine is possible under nonoxidative conditions. These results give insights into this important glycation reaction and provide a basis for future studies of the energetics and dynamics of these cross-linking processes.

**Table 2. Activation Barriers<sup>a</sup> (in kcal/mol at the CPCM/wB97XD/6-311++G\*\* Level of Theory) for Pathways A–E as a Function of the Number of Water Molecules**

	pentosidine				
	<i>n</i> = 1 <sup>b</sup>	<i>n</i> = 2	<i>n</i> = 3	<i>n</i> = 4	<i>n</i> = 5
pathway A					
TS10	42.9	31.6	37.9	26.1	31.1
TS11a	31.1	28.9	ND <sup>c</sup>	22.7	ND
TS11b	ND	35.2	ND	31.5	ND
TS13	40.5	34.5	ND	33.0	33.9
pathway B					
TS11	ND	63.2	60.6	59.6	58.9

<sup>a</sup>Refined free energies were determined relative to the relevant reactants. There were Int9, Int10, and Int13 for TS10, TS11, and TS13 in pathway A, respectively, and Int10 for TS11 in pathway B. <sup>b</sup>*n* is the number of added water molecules in the studied processes. <sup>c</sup>Not determined.

## ASSOCIATED CONTENT

### Supporting Information

Text, Cartesian coordinates, and Gibbs free energies for some stationary points are given. This material is available free of charge via the Internet at <http://pubs.acs.org>.

## AUTHOR INFORMATION

### Corresponding Author

\*E-mail: m-zahedi@cc.sbu.ac.ir. Tel: +98 21 22401765/29902889. Fax: +98 21 22401765/22431663.

### Notes

The authors declare no competing financial interest.

## ACKNOWLEDGMENTS

The financial support of Research Council of Shahid Beheshti University is gratefully acknowledged.

## REFERENCES

- Miyazaki, K.; Nagai, R.; Horiuchi, S. *J. Biochem. (Tokyo, Jpn.)* **2002**, *132*, 543–550.
- Sugiyama, S.; Miyata, T.; Ueda, Y.; Tanaka, H.; Maeda, K.; Kawashima, S.; Van Ypersele De Strihou, C.; Kurokawa, K. *J. Am. Soc. Nephrol.* **1998**, *9*, 1681–1688.
- (a) Miyata, T.; Ueda, Y.; Yamada, Y.; Izuohara, Y.; Wada, T.; Jadoul, M.; Saito, A.; Kurokawa, K.; Van Ypersele De Strihou, C. *Am. Soc. Nephrol.* **1998**, *9*, 2349–2356. (b) Miyata, T.; Van Ypersele De Strihou, C.; Kurokawa, K.; Baynes, J. W. *Kidney Int.* **1999**, *55*, 389–399. (c) Miyata, T.; Horie, K.; Ueda, Y.; Fujita, Y.; Izuohara, Y.; Hirano, H.; Uchida, K.; Saito, A.; Van Ypersele De Strihou, C.; Kurokawa, K. *Kidney Int.* **2000**, *58*, 425–435.
- Sternberg, Z.; Hennies, C.; Sternberg, D.; Bistolfi, G. L.; Kazim, L.; Benedict, R. H. B.; Chadha, K. *Mult. Scler.* **2011**, *17*, 157–163.
- Morales, S.; García-Salcedo, J. A.; Muñoz-Torres, M. *Med. Clin.* **2011**, *136*, 298–302.
- Kouda, K.; Nakamura, H.; Fan, W.; Horiuchi, K.; Takeuchi, H. *Clin. Biochem.* **2001**, *34*, 247–250.
- Hayase, F. *Food Sci. Technol. Res.* **2000**, *6*, 79–86.
- Peiretti, P. G.; Medana, C.; Visentini, S.; Giancotti, V.; Zunino, V.; Meineri, G. *Food Chem.* **2011**, *126*, 1939–1947.
- Sell, D. R.; Nagaraj, R. H.; Grandhee, S. K.; Odetti, P.; Lapolla, A.; Fogarty, J.; Monnier, V. M. *Diabetes* **1991**, *7*, 239–251.
- (a) Dyer, D. G.; Blackledge, J. A.; Thorpe, S. R.; Baynes, J. W. *J. Biol. Chem.* **1991**, *266*, 11654–11660. (b) Biemel, K. M.; Reihl, O.; Conrad, J.; Lederer, M. O. *J. Biol. Chem.* **2001**, *276*, 23405–23412. (c) Grandhee, S. K.; Monnier, V. M. *J. Biol. Chem.* **1991**, *266*, 11649–11653.
- Chellan, P.; Nagaraj, R. H. *J. Biol. Chem.* **2001**, *276*, 3895–3903.
- Farboud, B.; Aotaki-Keen, A.; Miyata, T.; Hjelmeland, L. M.; Handa, J. T. *Mol. Vision* **1999**, *5*, XI–XII.
- Litchfield, J. E.; Thorpe, S. R.; Baynes, J. W. *Int. J. Biochem. Cell Biol.* **1999**, *31*, 1297–1305.
- Lapolla, A.; Flamini, R.; Lupo, A.; Aricò, N. C.; Rugiu, C.; Reitano, R.; Tubaro, M.; Ragazzi, E.; Seraglia, E. R.; Traldi, P.; Ann, N. Y. *Acad. Sci.* **2005**, *1043*, 217–224.
- (a) Odani, H.; Shinzato, T.; Matsumoto, Y.; Usami, J.; Maeda, K. *Biochem. Biophys. Res. Commun.* **1999**, *256*, 89–93. (b) Thornalley, P. J. *Ann. N.Y. Acad. Sci.* **2005**, *1043*, 111–117.
- Frisch, M. J.; et al. *Gaussian 09*, Revision A.2; Gaussian, Inc.: Wallingford, CT, 2009; the full reference is given in the Supporting Information.
- Dennington, R. I.; Keith, T.; Millam, J. M.; Eppinnett, K.; Hovell, W. L.; Gilliland, R. *GaussView*, Version 3.07 ed.; Semichem, Inc.: Shawnee Mission, KS, 2003.
- Chai, J. D.; Head-Gordon, M. *Phys. Chem. Chem. Phys.* **2008**, *10*, 6615–20.
- (a) Gonzalez, C.; Schlegel, H. B. *J. Chem. Phys.* **1989**, *90*, 2154–2161. (b) Gonzalez, C.; Schlegel, H. B. *J. Phys. Chem.* **1990**, *94*, 5523–5527. (c) Barone, V.; Cossi, M. *J. Phys. Chem. A* **1998**, *102*, 1995–2001. (d) Cossi, M.; Rega, N.; Scalmani, G.; Barone, V. *J. Comput. Chem.* **2003**, *24*, 669–81.
- Martin, R. L.; Hay, P. J.; Pratt, L. R. *J. Phys. Chem. A* **1998**, *102*, 3565–3573.
- (a) Thornalley, P. J.; Langborg, A.; Minhas, H. S. *Biochem. J.* **1999**, *344*, 109–116. (b) Paul, R. G.; Avery, N. C.; Slatter, D. A.; Sims, T. J.; Bailey, A. J. *Biochem. J.* **1998**, *330*, 1241–1248.
- Brownlee, M.; Vlassara, H.; Kooney, A. *Science* **1986**, *232*, 1629–1632.
- Nakamura, S.; Makita, Z.; Ishikawa, S.; Yasumura, K.; Fujii, W.; Yanagisawa, K.; Kawata, T.; Koike, T. *Diabetes* **1997**, *46*, 895–899.
- (a) Rao, Q. Q.; Luo, S. W.; Gong, L. Z. *Chin. Sci. Bull.* **2010**, *55* (17), 1742–1752. (b) Dong, L.; Qin, S.; Su, Z.; Yang, H.; Hu, C. *Org. Biomol. Chem.* **2010**, *8*, 3985–3991.
- Brannock, K. C.; Bell, A.; Burpitt, R. D.; Kelly, C. A. *J. Org. Chem.* **1964**, *29*, 801–812.
- (a) Biemel, K. M.; Reihl, O.; Conrad, J.; Lederer, M. O. *J. Biol. Chem.* **2001**, *276*, 23405. (b) Biemel, K. M.; Friedl, D. A.; Lederer, M. O. *J. Biol. Chem.* **2002**, *277*, 24907–24915.
- Nasiri, R.; Zahedi, M.; Jamet, H.; Moosavi-Movahedi, A. A. *J. Mol. Model.* **2011**, *1–15*, DOI: 10.1007/s00894-011-1161-x.
- Nasiri, R.; Field, J. M.; Zahedi, M.; Moosavi-Movahedi, A. A. *J. Phys. Chem.* **2011**, *115*, 13542–13555.